Supplement of Atmos. Chem. Phys., 24, 7101–7121, 2024
https://doi.org/10.5194/acp-24-7101-2024-supplement

Atmospheric Chemistry and Physics
Open Access
EGU

Supplement of

Emission characteristics of reactive organic gases (ROGs) from industrial volatile chemical products (VCPs) in the Pearl River Delta (PRD), China

Sihang Wang et al.

Correspondence to: Bin Yuan (byuan@jnu.edu.cn)

Section S1. Detail information of test industrial volatile chemical product (VCP) sources

The shoemaking industry, as an important economic sector in developing countries, holds significance as one of the industrial VCP sources in the Pearl River Delta (PRD) region (Zheng et al., 2013;Estevan et al., 2012). Reactive organic gases (ROGs) emissions in this industry primarily originate from the extensive use of industrial adhesives, which compositions predominantly consist of butanone, acetone, cyclohexane, and ethyl acetate (Zheng et al., 2013;Zhao et al., 2018;Estevan et al., 2012). The factories involved in this study primarily specialize in producing leather shoes, high-heeled shoes, and other footwear products, with the bottom forming process serving as the primary source of ROG emissions.

In the production of various daily necessities including electronic products and auto parts, the process of plastic surface coating plays a crucial role. Raw materials of plastic are nylon, polypropylene, and polycarbonate, and the industrial water-borne coatings was mainly used to spray in this industry. As a representative industry in this study, a plastic toy factory specializing in the production of plastic toys and electronic toys was selected. The main processes contributing to ROG emissions in this factory were manual and automatic spraying (workshop A (manual-spray workshop) and workshop B (auto-spray workshop) in Fig 1b). The concentration of oxygenated ROG species (OVOCs) showed marginal increase after treatment (Fig. S7), only C_8 aromatics exhibited a slight decrease. This could be due to the fact that the adsorption materials used in the ROG treatment devices may not be effective for all ROGs, necessitating timely replacement and underscoring the importance of ROGs removal by treatment devices.

The furniture coating industry is recognized as a significant sector for the prevention and control of ROGs in China due to its outdated technology, low pollution control levels, and high ROG emissions (Zheng et al., 2013). Due to the extensive use of industrial coatings (including water-borne and solvent-borne coatings) in the furniture coating industry, ROG emissions mainly come from the primer and topcoat

processes (Zhou et al., 2020;Zheng et al., 2013;Fang et al., 2019). As the representative industry in this study, a wood furniture coating factory was selected where topcoat spraying emerged as the primary source of ROG emissions. The discrepancy between ROG concentrations before and after treatment indicates that the ROGs treatment device was ineffective in this factory, possibly due to device malfunction or insufficient replacement of adsorption materials in a timely manner.

The printing industry employs various printing techniques, including offset, gravure, letterpress, and digital, to produce a wide range of printed products, such as books, brochures, packaging, and labels (Zheng et al., 2013). ROG emissions from this industry were mainly derived from the industrial inks utilized in the printing production (Zhou et al., 2020;Zheng et al., 2013;Fang et al., 2019). In this study, a comprehensive printing factory encompassing packaging and digital printing was selected as the representative industry, with ROG emissions are generated through the use of industrial inks during the manufacturing process.

As one of the important ports and shipbuilding bases in China, the PRD region has a solid foundation in the shipbuilding industry. Utilization of solvent-borne industrial coatings for ship coating remains prevalent due to stringent requirements for anti-rust and anti-corrosion properties. The cost-effectiveness and superior efficiency of solvent-borne industrial coatings outweigh the preference for water-borne industrial coatings alternative (Malherbe and Mandin, 2007). For this study, a large ship coating factory was selected as a representative industry, with ROG emissions primarily occurring during the coating spraying process. Since the coating spraying process is limited to a single workshop, we conducted three repeated experiments at the same sampling point (workshops and after treatment device) to validate our test results (Fig. S6b). It was observed that the concentrations of typical ROGs during the second and third sampling were consistent and stable, indicating the stability of waste gas collection and power generation by the ROGs treatment device. Conversely, the fluctuating concentrations observed during the initial sampling could be attributed to the fresh start of the coating spraying process in the factory or the preheating state of the ROGs

74 treatment device.

75 Section S2. The fractions of ROGs in total ROG emissions

76 Combined with the measurements of canisters measured by gas chromatography-
77 mass spectrometer/flame ionization detector (canister-GC-MS/FID) and proton transfer
78 reaction time-of-flight mass spectrometer based on H_3O^+ and NO^+ chemical ionization
79 (H_3O^+/NO^+ PTR-ToF-MS), more comprehensive speciation of ROG emissions from
80 industrial VCP sources had been characteristic, and the fractions of ROGs in total ROG
81 emissions can be determined for various industrial VCP sources.

82 In this study, a more comprehensive speciation of ROGs was achieved by the
83 combination of GC-MS/FID and PTR-ToF-MS, the same ROG species from the
84 combination measurement should be counted only once. All ROG species detected in
85 this study is summarized in Table S2. Specifically, to facilitate comparison with
86 traditional photochemical assessment monitoring stations (PAMS) species, C_6-C_{10}
87 aromatics were identified using GC/MS-FID, while C_{10}-C_{12} alkanes were detected
88 using NO^+ PTR-ToF-MS, as GC-MS/FID only containing the n-alkanes. For unknown
89 ROG species, we used the semi-quantity based on the methods.

90 As shown in Fig. S5, we compared concentrations of toluene and C_8 aromatics
91 from the offline canister-GC-MS/FID and the online H_3O^+/NO^+ PTR-ToF-MS,
92 obtaining generally consistent results, considering the large variation in ROG emissions
93 for manufacturing processes conditions and the difficulty to control the fill time for
94 canisters. Due to the results of toluene and C_8 aromatics from H_3O^+ PTR-ToF-MS and
95 the offline canister-GC-MS/FID were consistent in our previous emission source
96 campaign (Wang et al., 2022), the ROGs/toluene ratio and ROGs/C_8 aromatics ratio
97 were used to evaluate the fractions of ROGs in total ROG emissions. Specifically,
98 ROGs/toluene ratio was used in shoemaking and printing industries, and ROGs/C_8
99 aromatics ratio was used in plastic surface coating, furniture coating, and ship coating
100 industries, considering the real-time concentrations of toluene and C_8 aromatics in
101 various industries, and the consistency between offline canister GC-MS/FID and

H_3O^+/NO^+ PTR-ToF-MS (Fig. S5). The fractions were calculated as Equation (1) and (2):

$$Fraction_{ROGs,i} = \frac{\frac{C_{ROGs,i}}{C_{toluene,PTR}}}{\left(\sum\frac{C_{ROGs,i}}{C_{toluene,PTR}}+\sum\frac{C_{other\ ROGs,i}}{C_{toluene,GC}}\right)} * 100\% \quad (1)$$

$$Fraction_{ROGs,i} = \frac{\frac{C_{ROGs,i}}{C_{C8\ Aromatics,PTR}}}{\left(\sum\frac{C_{ROGs,i}}{C_{C8\ Aromatics,PTR}}+\sum\frac{C_{other\ ROGs,i}}{C_{C8\ Aromatics,GC}}\right)} * 100\% \quad (2)$$

Where $Fraction_{ROGs,i}$ is the fraction of ROGs, i; $C_{ROGs,i}$, $C_{toluene,PTR}$, and $C_{C8\ Aromatics,PTR}$ are the concentrations of ROGs, i, toluene, and C_8 aromatics measured by H_3O^+ PTR-ToF-MS. $C_{other\ ROGs,i}$, $C_{toluene,GC}$, and $C_{C8\ Aromatics,GC}$ are the concentrations of other ROGs, i, toluene, and C_8 aromatics measured by offline canister-GC-MS/FID, and the concentration of C_8 aromatics was the total concentration of ethylbenzene, o-xylene, and m/p-xylene.

Supplement tables

Table S1. Detailed information of the test industrial VCP sources in this study.

Industrial VCP sources	Sampling location	samples
Shoemaking	Semi-open workshops	3
	Before treatment	1
	After treatment (stack)	1
Plastic surface coating	Semi-open workshops	5
	Before treatment	3
	After treatment (stack)	2
Furniture coating	Semi-open workshops	5
	Before treatment	1
	After treatment (stack)	1
Printing	Semi-open workshops	4
	Before treatment	3
	After treatment (stack)	2
Ship coating	Semi-open workshops	3
	Before treatment	-
	After treatment (stack)	3

Table S2. Detailed information of ROG species measured by different instruments.

Components	Measurements	ROG species
OVOCs	PTR-H_3O^+	formula only including CHO
N/S-containing	PTR-H_3O^+	formula including CHN, CHS, CHON, CHOS, and CHONS
Heavy aromatics and monoterpenes	PTR-H_3O^+	monoterpenes, C_{11}-C_{20} aromatics and polynuclear aromatic hydrocarbons (PAHs)
Higher alkanes	PTR-NO^+	C_{10}-C_{20} acyclic, cyclic and bicyclic alkanes
Alkanes	GC-MS/FID	C_2-C_9 alkanes
Alkenes	GC-MS/FID	C_2-C_6 alkenes
Aromatics	GC-MS/FID	C_6-C_{10} aromatics
Halohydrocarbons	GC-MS/FID	C_1-C_6 halohydrocarbons

Table S3. Sensitivities of H_3O^+ PTR-ToF-MS for various ROGs calibrated with standard gas.

ROGs	Ion formula (H^+)	Sensitivity, cps·ppb^{-1}
Species calibrated with standard gas		
HCN	$HCNH^+$	630.86
Formaldehyde	CH_2OH^+	1063.76
Methanol	CH_4OH^+	757.38
Acetonitrile	$C_2H_3NH^+$	3006.75
Acetaldehyde	$C_2H_4OH^+$	3782.23
Ethanol	$C_2H_6OH^+$	131.58
Acrolein	$C_3H_4OH^+$	4097.50
Acetone	$C_3H_6OH^+$	4943.88
Isopropanol	$C_3H_8OH^+$	-
Furan	$C_4H_4OH^+$	2993.73
Isoprene	$C_5H_8H^+$	1589.89
MVK	$C_4H_6OH^+$	3396.10
MEK	$C_4H_8OH^+$	4089.86
Hydroxy acetone	$C_3H_6O_2H^+$	3172.43
Benzene	$C_6H_6H^+$	3629.18
2-Pentanone	$C_5H_{10}OH^+$	4120.96
Ethyl acetate	$C_4H_8O_2H^+$	959.96
Toluene	$C_7H_8H^+$	4584.74
Phenol	$C_6H_6OH^+$	5064.30
Furfural	$C_5H_4O_2H^+$	10109.39
Methyl Isobutyl Ketone	$C_6H_{12}OH^+$	3446.37
Styrene	$C_8H_8H^+$	5858.41
o-Xylene	$C_8H_{10}H^+$	4883.79
m-Cresol	$C_7H_8OH^+$	5191.14
1,2,4-Teimethylbenzene	$C_9H_{12}H^+$	5337.79
Guaiacol	$C_7H_8O_2H^+$	7090.09
Naphthalene	$C_{10}H_8H^+$	7485.81
a-Pinene	$C_{10}H_{16}H^+$	1626.14
Chlorobenzene	$C_6H_5ClH^+$	5084.49
1,3-Dichlorobenzene	$C_6H_4Cl_2H^+$	6314.09
1,3,5-Trichlorobenzene	$C_6H_3Cl_3H^+$	8130.16
D3 Siloxane	$C_6H_{18}O_3Si_3H^+$	3620.62
D4 Siloxane	$C_8H_{24}O_4Si_4H^+$	3236.92
D5 Siloxane	$C_{10}H_{30}O_5Si_5H^+$	2991.05

Table S4. Sensitivities of NO^+ PTR-ToF-MS for alkanes and cycloalkanes calibrated with standard gas.

ROGs	Formula	Sensitivity, ncps·ppb^{-1}
Species calibrated with standard gas		
C_8 Alkanes	C_8H_{18}	99.79
C_9 Alkanes	C_9H_{20}	79.91
C_{10} Alkanes	$C_{10}H_{22}$	68.27
C_{11} Alkanes	$C_{11}H_{24}$	68.13
C_{12} Alkanes	$C_{12}H_{26}$	77.43
C_{13} Alkanes	$C_{13}H_{28}$	104.81
C_{14} Alkanes	$C_{14}H_{30}$	140.81
C_{15} Alkanes	$C_{15}H_{32}$	164.34
C_{10} cyclic alkanes	$C_{10}H_{20}$	137.54
C_{11} cyclic alkanes	$C_{11}H_{22}$	119.71
C_{12} cyclic alkanes	$C_{12}H_{24}$	131.94
C_{13} cyclic alkanes	$C_{13}H_{26}$	147.60
C_{14} cyclic alkanes	$C_{14}H_{28}$	150.12
C_{15} cyclic alkanes	$C_{15}H_{30}$	137.38 [a]

[a]: The average sensitivity of C_{10}–C_{14} cyclic alkanes was used to predict the concentrations of cyclic alkanes with higher carbon (C_{15}–C_{20}) and bicyclic alkanes (C_{10}–C_{20}) (Chen et al., 2022).

136 **Table S5.** Sensitivities of H_3O^+ PTR-ToF-MS for various ROGs calibrated with liquid
137 calibration unit (LCU).
138

ROGs	Ion formula	Sensitivity, cps·ppb^{-1}
Species calibrated with liquid calibration unit (LCU)		
Formic acid	$CH_2O_2H^+$	939.43
Acetic acid	$C_2H_4O_2H^+$	1876.45
Propionic acid	$C_3H_6O_2H^+$	2272.36
Butyric acid	$C_4H_8O_2H^+$	3531.01
Pyrrole	$C_4H_5NH^+$	3219.67
Formamide	CH_3NOH^+	3567.04
Acetamide	$C_2H_5NOH^+$	4959.81
Catechol	$C_6H_6O_2H^+$	2035.52
Guaiacol	$C_7H_8O_2H^+$	5989.24
2-Nitrophenol	$C_6H_5NO_3H^+$	4469.34
2-Nitro-p-Cresol	$C_7H_7NO_3H^+$	2335.15

139
140

Table S6. The formula and purity of the chemicals used in characteristic product ion recognition experiment are shown. Product ions of the reactions of H_3O^+ and NO^+ ions with their percentages of each indicated in brackets.

Chemicals	Formula	Purity (%)	Mode	Product ions (%)		
Methyl acetate	$C_3H_6O_2$	99.9%	H_3O^+	**$C_3H_6O_2H^+$ (94.8)**	$C_2H_4O_2H^+$ (0.5)	$C_2H_2OH^+$ (4.7)
Ethyl acetate	$C_4H_8O_2$	99.9%	H_3O^+	**$C_4H_8O_2H^+$ (72.4)**	$C_2H_4O_2H^+$ (22.2)	$C_2H_2OH^+$ (5.4)
Isopropyl acetate	$C_5H_{10}O_2$	99.9%	H_3O^+	$C_5H_{10}O_2H^+$ (12.7)	**$C_2H_4O_2H^+$ (73.5)**	$C_2H_2OH^+$ (13.8)
Vinyl acetate	$C_4H_6O_2$	99.9%	H_3O^+	**$C_4H_6O_2H^+$** (19.5)	$C_2H_4O_2H^+$ (2.1)	$C_2H_2OH^+$ (78.4)
Methyl acetate	$C_3H_6O_2$	99.9%	NO^+	**$C_3H_6O_2NO^+$ (82.6)**	$C_3H_6O_2H^+$ (14.0)	$C_3H_6O_2(H_2O)H^+$ (3.4)
Ethyl acetate	$C_4H_8O_2$	99.9%	NO^+	**$C_4H_8O_2NO^+$ (80.0)**	$C_4H_8O_2H^+$ (17.4)	$C_4H_8O_2(H_2O)H^+$ (2.6)
Vinyl acetate	$C_4H_6O_2$	99.9%	NO^+	$C_4H_6O_2NO^+$ (0.3)	$C_4H_6O_2H^+$ (6.5)	$C_4H_6O_2(H_2O)H^+$ (1.5)
				$C_2H_2OH^+$ (46.9)	$C_2H_4O_2H^+$ (20.4)	$C_2H_4O_2(H_2O)H^+$ (24.4)
Acetone	C_3H_6O	99.7%	NO^+	**$C_3H_6ONO^+$ (77.2)**	$C_3H_6OH^+$ (22.8)	
isoPropanol	C_3H_8O	99.5%	NO^+	**$C_3H_7O^+$ (88.1%)**	$C_3H_8OH^+$ (4.1)	$C_3H_7O(H_2O)^+$ (3.7)
				$C_3H_6H^+$ (2.5)	$C_3H_8O(H_2O)H^+$ (1.6)	

147 **Table S7.** The θ angles (°) among the mass spectra of industrial VCP sources in this
148 study and vehicular emissions from previous study (Wang et al., 2022).
149

ROG sources	Shoe making	plastic surface coating	Furniture coating	Printing	Ship coating	Gasoline vehicle	Diesel vehicle	LPG vehicle
Shoemaking	0	61.8	67.6	74.3	85.6	83.0	78.6	78.2
plastic surface coating		0	75.1	27.4	88.9	88.7	81.1	81.9
Furniture coating			0	82.6	63.4	73.3	70.0	71.6
Printing				0	89.7	89.5	86.9	86.7
Ship coating					0	51.1	80.7	72.2
Gasoline						0	74.8	67.8
Diesel							0	41.2
LPG								0

150

151

Table S8. The θ angles (°) among the mass spectra of different workshops in industrial VCP sources.

(a) Shoemaking industry workshops angles (°)

No.	1	2	3
1	0.00	24.88	60.26
2		0.00	52.35
3			0.00

(b) Plastic surface coating industry workshops angles (°)

No.	1	2	3	4	5
1	0.00	20.65	13.60	40.60	46.03
2		0.00	18.18	36.69	31.94
3			0.00	40.73	45.86
4				0.00	44.20
5					0.00

(c) Furniture coating industry workshops angles (°)

No.	1	2	3	4	5
1	0.00	21.60	29.45	36.38	26.01
2		0.00	19.77	22.57	13.43
3			0.00	14.13	14.53
4				0.00	19.04
5					0.00

(d) Printing industry workshops angles (°)

No.	1	2	3	4
1	0.00	2.47	6.52	5.88
2		0.00	7.57	6.99
3			0.00	2.09
4				0.00

(e) Ship coating industry workshops angles (°)

No.	1	2	3
1	0.00	9.04	7.96
2		0.00	1.58
3			0.00

Table S9. The θ angles (°) among the mass spectra of different emission standards from vehicular emissions.

(a) Gasoline vehicle angles (°)

Emission standard	China I	China II	China III	China IV	China V	China VI
China I	0.00	6.12	6.58	10.36	9.63	16.83
China II		0.00	4.85	8.39	7.18	13.21
China III			0.00	9.48	5.68	13.71
China IV				0.00	6.21	13.32
China V					0.00	11.79
China VI						0.00

(b) Light-duty diesel truck angles (°)

Emission standard	China III	China IV	China V
China III	0.00	17.71	49.38
China IV		0.00	45.28
China V			0.00

(c) Middle-duty diesel truck angles (°)

Emission standard	China III	China IV	China V
China III	0.00	38.56	63.77
China IV		0.00	31.08
China V			0.00

(d) Heavy-duty diesel truck angles (°)

Emission standard	China III	China IV	China V
China III	0.00	71.21	65.05
China IV		0.00	18.41
China V			0.00

Table S10. Weight percentage (%) of ROG components to total ROG emissions at workshops and stack (after-treatment) from shoemaking, plastic surface coating, furniture coating, printing, and ship coating industries.

Weight percentage (%)		Shoemaking		Plastic surface coating		Furniture coating		Printing		Ship coating	
Components	Measurement	Workshops	Stack	Workshops	Stack	Workshops	Stack	Workshops	Stack	Workshops	Stack
OVOCs	PTR-H_3O^+	47.6±12.5	67.1	63.3±21.2	96.1±0.2	66.9±5.1	76.8	61.0±1.5	84.6±6.5	10.6±2.8	16.4±3.5
N/S-containing	PTR-H_3O^+	0.1±0.1	0.1	0.1±0.0	0.3±0.1	0.1±0.0	0.0	0.0±0.0	0.1±0.0	0.1±0.0	0.1±0.0
Si/Cl-containing [a]	PTR-H_3O^+	0.1±0.1	0.0	0.0±0.0	0.0±0.0	0.0±0.0	0.0	0.0±0.0	0.0±0.0	0.0±0.0	0.0±0.0
Heavy aromatics and monoterpenes [b]	PTR-H_3O^+	0.2±0.0	0.0	0.1±0.1	0.3±0.0	0.3±0.1	0.3	0.1±0.1	0.0±0.0	1.2±0.3	1.3±0.1
Higher alkanes [c]	PTR-NO^+	2.0±0.3	0.0	0.8±0.6	0.1±0.1	0.3±0.4	0.1	27.0±2.7	8.2±2.4	1.9±1.1	6.5±2.1
Alkanes	GC-MS/FID	24.7±1.4	26.1	23.4±18.6	2.2±0.5	3.4±0.6	0.5	5.3±4.1	1.4±1.3	1.3±0.4	0.6±0.2
Alkenes	GC-MS/FID	0.6±0.4	0.1	0.3±0.1	0.1±0.1	0.1±0.0	0.0	0.1±0.0	0.9±1.2	0.1±0.0	0.0±0.0
Aromatics	GC-MS/FID	17.4±6.0	6.1	7.2±1.6	0.4±0.4	26.3±5.6	22.1	4.5±4.5	0.7±0.2	83.5±2.3	73.7±6.1
Halohydrocarbons	GC-MS/FID	7.3±4.8	0.5	4.8±1.6	0.5±0.3	2.6±0.3	0.2	1.9±1.5	4.2±4.0	1.4±0.1	1.5±0.6

[a]: Si/Cl-containing including D_3-D_6 siloxanes and chlorobenzenes.

[b]: Heavy aromatics and monoterpenes including monoterpenes, C_{11}-C_{20} aromatics and PAHs such as naphthalene, methylnaphthalene etc.

[c]: Higher alkanes including C_{10}-C_{20} acyclic, cyclic and bicyclic alkanes.

Table S11. Fractions of ROG components to total OH reactivity (OHR) of ROGs at workshops and stack (after-treatment) in shoemaking, plastic surface coating, furniture coating, printing, and ship coating industries.

Fraction (%)		Shoemaking		Plastic surface coating		Furniture coating		Printing		Ship coating	
Components	Measurement	Workshops	Stack	Workshops	Stack	Workshops	Stack	Workshops	Stack	Workshops	Stack
OVOCs	PTR-H_3O^+	44.4±16.7	72.1	62.3±19.8	97.3±0.6	78.0±3.8	87.7	58.0±6.9	84.5±6.9	8.1±2.6	15.1±3.6
N/S-containing	PTR-H_3O^+	0.2±0.1	0.1	0.0±0.0	0.0±0.0	0.0±0.0	0.0	0.0±0.1	0.1±0.1	0.0±0.0	0.0±0.0
Si/Cl-containing [a]	PTR-H_3O^+	0.0±0.0	0.0	0.0±0.0	0.0±0.0	0.0±0.0	0.0	0.0±0.0	0.0±0.0	0.0±0.0	0.0±0.0
Heavy aromatics and monoterpenes [b]	PTR-H_3O^+	1.5±0.3	0.1	0.4±0.4	0.1±0.0	0.9±0.1	0.1	0.6±0.4	0.2±0.1	3.2±0.6	3.8±0.4
Higher alkanes [c]	PTR-NO^+	1.7±0.5	0.0	0.7±0.5	0.1±0.1	0.1±0.1	0.1	30.1±2.4	9.0±2.0	0.8±0.5	1.8±0.9
Alkanes	GC-MS/FID	18.3±0.5	20.2	19.3±17.7	1.3±0.4	1.2±0.1	0.1	3.3±2.4	0.9±0.9	0.6±0.2	0.3±0.1
Alkenes	GC-MS/FID	3.6±2.7	0.6	2.3±0.9	0.3±0.3	0.5±0.0	0.0	0.6±0.2	4.4±6.1	0.3±0.1	0.1±0.0
Aromatics	GC-MS/FID	30.4±14.6	6.9	15.1±2.1	0.8±0.7	19.4±3.9	12.1	7.4±7.5	0.9±0.2	87.0±2.8	79.0±4.8

[a]: Si/Cl-containing are including D_3-D_6 siloxanes and chlorobenzenes.

[b]: Heavy aromatics and monoterpenes are including monoterpenes, C_{11}-C_{20} aromatics and PAHs such as naphthalene, methylnaphthalene etc.

[c]: Higher alkanes are including C_{10}-C_{20} acyclic, cyclic and bicyclic alkanes.

Table S12. Fractions of the top ten most abundant species in total ROG emissions, total OHR, and total ozone formation potential (OFP) from (a) shoemaking, (b) plastic surface coating, (c) furniture coating, (d) printing, and (e) ship coating industries.

(a) Shoemaking

num	Concentration			OH reactivity			OFP		
	species name	formula	fraction (%)	species name	formula	fraction (%)	species name	formula	fraction (%)
1	Isopentane	C5H12	24.39	isoPropanol	C3H8O	27.32	Isopentane	C5H12	24.53
2	MEK	C4H8O	21.36	MEK	C4H8O	24.73	MEK	C4H8O	21.94
3	isoPropanol	C3H8O	20.54	Isopentane	C5H12	18.53	Toluene	C7H8	15.22
4	Acetone	C3H6O	12.64	Formaldehyde	CH2O	9.93	Formaldehyde	CH2O	13.98
5	Ethyl acetate	C4H8O2	6.19	Toluene	C7H8	5.10	isoPropanol	C3H8O	8.69
6	Toluene	C7H8	5.48	Ethyl acetate	C4H8O2	1.91	Acetone	C3H6O	3.16
7	Formaldehyde	CH2O	2.13	Butanediol	C4H10O2	1.35	Ethyl acetate	C4H8O2	2.70
8	Dimethyl carbonate	C3H6O3	0.80	MTBE	C5H12O	1.02	Glyoxal	C2H2O2	1.03
9	Methyl acetate	C3H6O2	0.62	Acetaldehyde	C2H4O	0.73	Acetaldehyde	C2H4O	0.65
10	Ethanol	C2H6O	0.55	Acetone	C3H6O	0.66	Methyl glyoxal	C3H4O2	0.61
	Total fraction		94.71			91.29			92.52

(b) Plastic surface coating

num	Concentration			OH reactivity			OFP		
	species name	formula	fraction (%)	species name	formula	fraction (%)	species name	formula	fraction (%)
1	isoPropanol	C3H8O	45.89	isoPropanol	C3H8O	54.16	isoPropanol	C3H8O	25.41
2	Acetone	C3H6O	16.41	Formaldehyde	CH2O	12.64	Formaldehyde	CH2O	25.08
3	Cyclohexanone	C6H10O	14.08	Cyclohexanone	C6H10O	10.24	Cyclohexanone	C6H10O	17.02
4	Butyl acetate	C6H12O2	3.52	Acetaldehyde	C2H4O	4.99	Acetaldehyde	C2H4O	6.61
5	Formaldehyde	CH2O	3.00	Butyl acetate	C6H12O2	2.12	Acetone	C3H6O	5.29
6	Methyl acetate	C3H6O2	2.85	Dimethyl furan	C6H8O	1.08	Butyl acetate	C6H12O2	2.62

7	Methanol	CH4O	2.10	Furan	C4H4O	1.07	Glyoxal	C2H2O2	2.17
8	Isopentane	C5H12	1.59	Allyl acetate	C5H6O2	0.98	Isopentane	C5H12	2.06
9	Ethyl acetate	C4H8O2	1.44	Isopentane	C5H12	0.93	MVK+MACR	C4H6O	1.52
10	Acetaldehyde	C2H4O	1.13	Methyl furan	C5H6O	0.87	Methanol	CH4O	1.26
	Total fraction		92.01			89.09			89.04

(c) Furniture coating

num	Concentration			OH reactivity			OFP		
	species name	formula	fraction (%)	species name	formula	fraction (%)	species name	formula	fraction (%)
1	MEK	C4H8O	13.01	Acetylacetone	C5H8O2	30.28	m/p-Xylene	C8H10	31.06
2	m/p-Xylene	C8H10	10.88	2-ethyl-1,3-hexanediol	C8H18O2	26.34	o-Xylene	C8H10	13.41
3	Acetylacetone	C5H8O2	8.68	m/p-Xylene	C8H10	7.10	MEK	C4H8O	7.04
4	Butyl acetate	C6H12O2	6.19	Tetralone	C10H10O	4.37	Butyl lactate	C7H14O3	5.05
5	Butyl lactate	C7H14O3	6.06	MEK	C4H8O	4.18	Hexanone	C6H12O	4.77
6	Ethyl acetate	C4H8O2	5.80	Butyl Lactate	C7H14O3	4.03	Ethyl benzene	C8H10	4.36
7	PGMEA	C6H12O3	4.85	Hexanone	C6H12O	3.26	Formaldehyde	CH2O	4.03
8	o-Xylene	C8H10	4.80	o-Xylene	C8H10	2.25	Vinyl Acetate	C4H6O2	3.93
9	Hexanone	C6H12O	4.15	Vinyl Acetate	C4H6O2	2.11	Acetylacetone	C5H8O2	3.21
10	Tetralone	C10H10O	4.07	PGMEA	C6H12O3	1.53	1,2,4-TMB	C9H12	2.65
	Total fraction		68.47			85.46			79.50

(d) Printing

num	Concentration			OH reactivity			OFP		
	species name	formula	fraction (%)	species name	formula	fraction (%)	species name	formula	fraction (%)
1	isoPropanol	C3H8O	73.43	isoPropanol	C3H8O	74.66	isoPropanol	C3H8O	56.77
2	Ethyl acetate	C4H8O2	5.38	C14 cycloalkanes	C14H28	4.23	1-Pentene	C5H10	7.33
3	Methylene chloride	CH2Cl2	4.06	1-Pentene	C5H10	4.05	Formaldehyde	CH2O	5.06
4	C14 cycloalkanes	C14H28	3.46	Acetaldehyde	C2H4O	2.30	Acetaldehyde	C2H4O	4.91
5	Ethanol	C2H6O	2.16	C13 cycloalkanes	C13H26	2.19	Ethyl acetate	C4H8O2	4.30

6	C13 cycloalkanes	C13H26	1.78	Ethanol	C2H6O	1.71	Ethanol	C2H6O	4.19
7	C15 cycloalkanes	C15H32	1.06	Formaldehyde	CH2O	1.49	C14 cycloalkanes	C14H28	2.85
8	Acetone	C3H6O	0.95	Ethyl acetate	C4H8O2	1.29	Toluene	C7H8	1.88
9	1-Pentene	C5H10	0.80	C15 cycloalkanes	C15H32	1.06	C13 cycloalkanes	C13H26	1.58
10	n-Pentane	C5H12	0.78	MTBE	C5H12O	0.81	n-Pentane	C5H12	1.29
	Total fraction		93.86			93.79			90.16

(e) Ship coating

num	Concentration			OH reactivity			OFP		
	species name	formula	fraction (%)	species name	formula	fraction (%)	species name	formula	fraction (%)
1	m/p-Xylene	C8H10	38.78	m/p-Xylene	C8H10	51.32	m/p-Xylene	C8H10	55.46
2	Ethyl benzene	C8H10	21.12	o-Xylene	C8H10	14.25	o-Xylene	C8H10	20.96
3	o-Xylene	C8H10	14.96	Ethyl benzene	C8H10	10.35	Ethyl benzene	C8H10	11.77
4	MEK	C4H8O	9.55	MEK	C4H8O	5.94	MEK	C4H8O	2.59
5	Methanol	CH4O	3.20	Acetaldehyde	C2H4O	3.28	Acetaldehyde	C2H4O	1.43
6	1,2-Dichloroethane	C2H4Cl2	1.32	C11 Aromatics	C11H16	2.87	Formaldehyde	CH2O	1.17
7	Acetaldehyde	C2H4O	1.19	Formaldehyde	CH2O	1.69	1,2,4-TMB	C9H12	1.03
8	C11 Aromatics	C11H16	1.04	1,2,4-TMB	C9H12	1.27	C11 Aromatics	C11H16	1.03
9	Ethanol	C2H6O	0.88	Acrolein	C3H4O	1.05	Acrolein	C3H4O	0.49
10	Formaldehyde	CH2O	0.68	Methanol	CH4O	0.64	m-Ethyltoluene	C9H12	0.45
	Total fraction		92.70			92.66			96.38

Table S13. The θ angles (°) among the mass spectra of workshops, before and after treatment in industrial VCP sources.

Industrial VCP sources	Sites	Workshops	Before treatment	After treatment
Shoemaking	Workshops	0.0	40.9	49.2
	Before treatment	40.9	0.0	27.0
	After treatment	49.2	27.0	0.0
Plastic surface coating	Workshops	0.0	26.0	15.6
	Before treatment	26.0	0.0	13.6
	After treatment	15.6	13.6	0.0
Furniture coating	Workshops	0.0	8.3	12.5
	Before treatment	8.3	0.0	7.5
	After treatment	12.5	7.5	0.0
Printing	Workshops	0.0	4.2	6.2
	Before treatment	4.2	0.0	2.5
	After treatment	6.2	2.5	0.0
Ship coating	Workshops	0.0		7.6
	After treatment	7.6		0.0

Supplement figures

Figure S1. A (a) mobile monitoring vehicle was parking equipped with (b) online measurement instruments at a fixed site which close to (c) the sampling ports of semi-open workshops and (d) stack emissions.

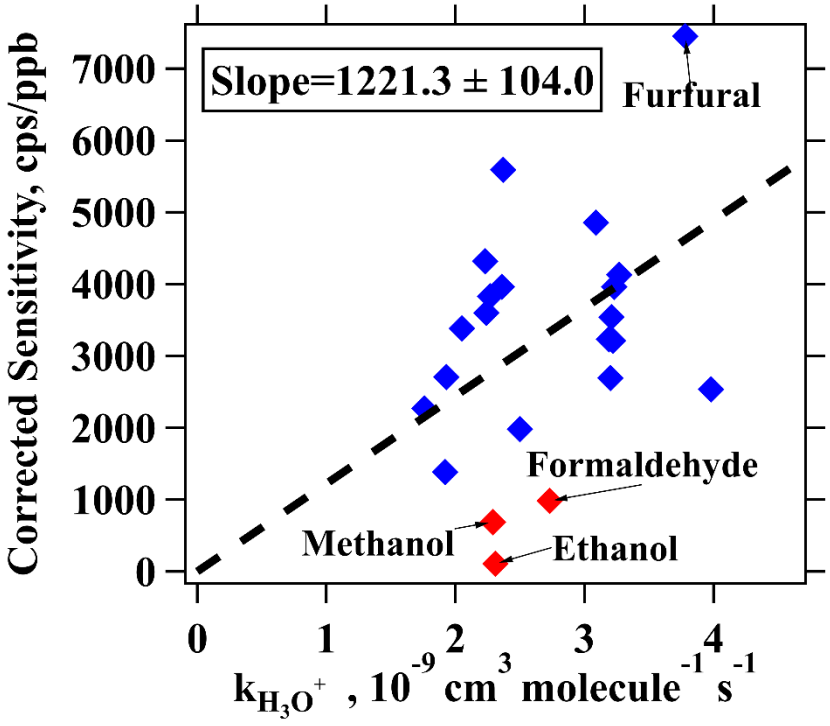

Figure S2. Corrected sensitivities as a function of kinetic rate constants for proton transfer reactions of H_3O^+ with ROGs. The dashed line indicates the fitted line for blue points. The red points not used as these compounds (formaldehyde, methanol, and ethanol) are known to have lower sensitivities.

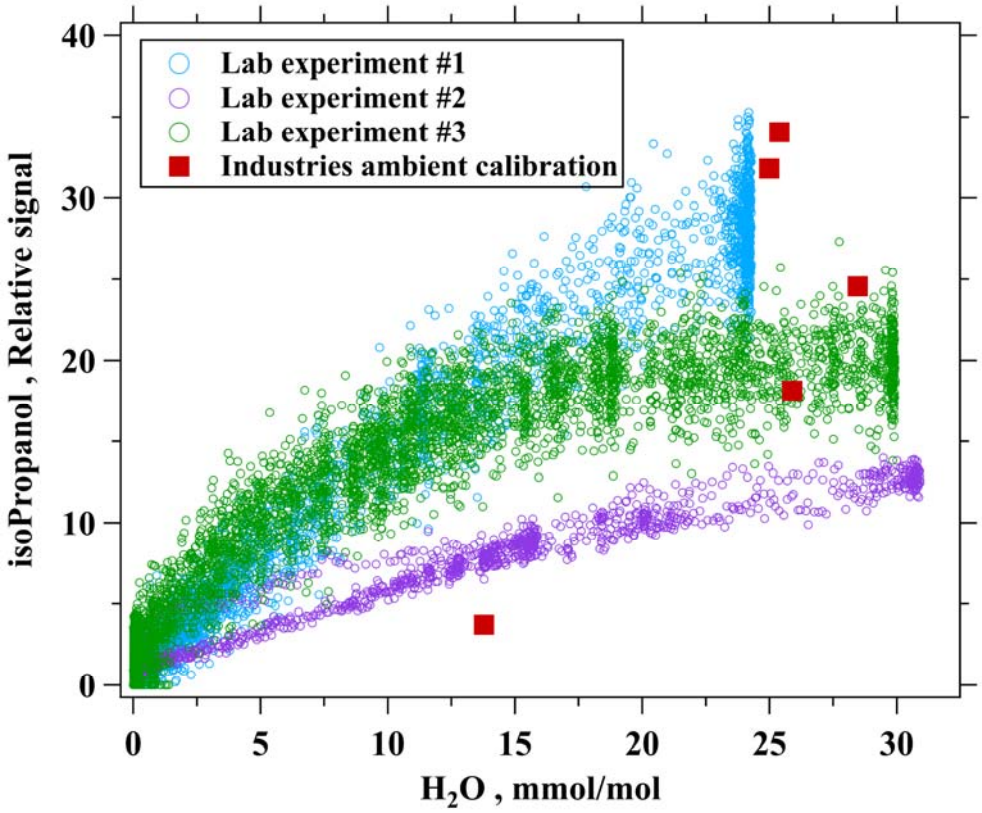

Figure S3. Humidity dependence of relative signal (wet versus dry) of isopropanol, including results in lab experiments (blue, green, and purple markers) and calibration the under ambient humidity conditions during the field campaign in this study (red markers).

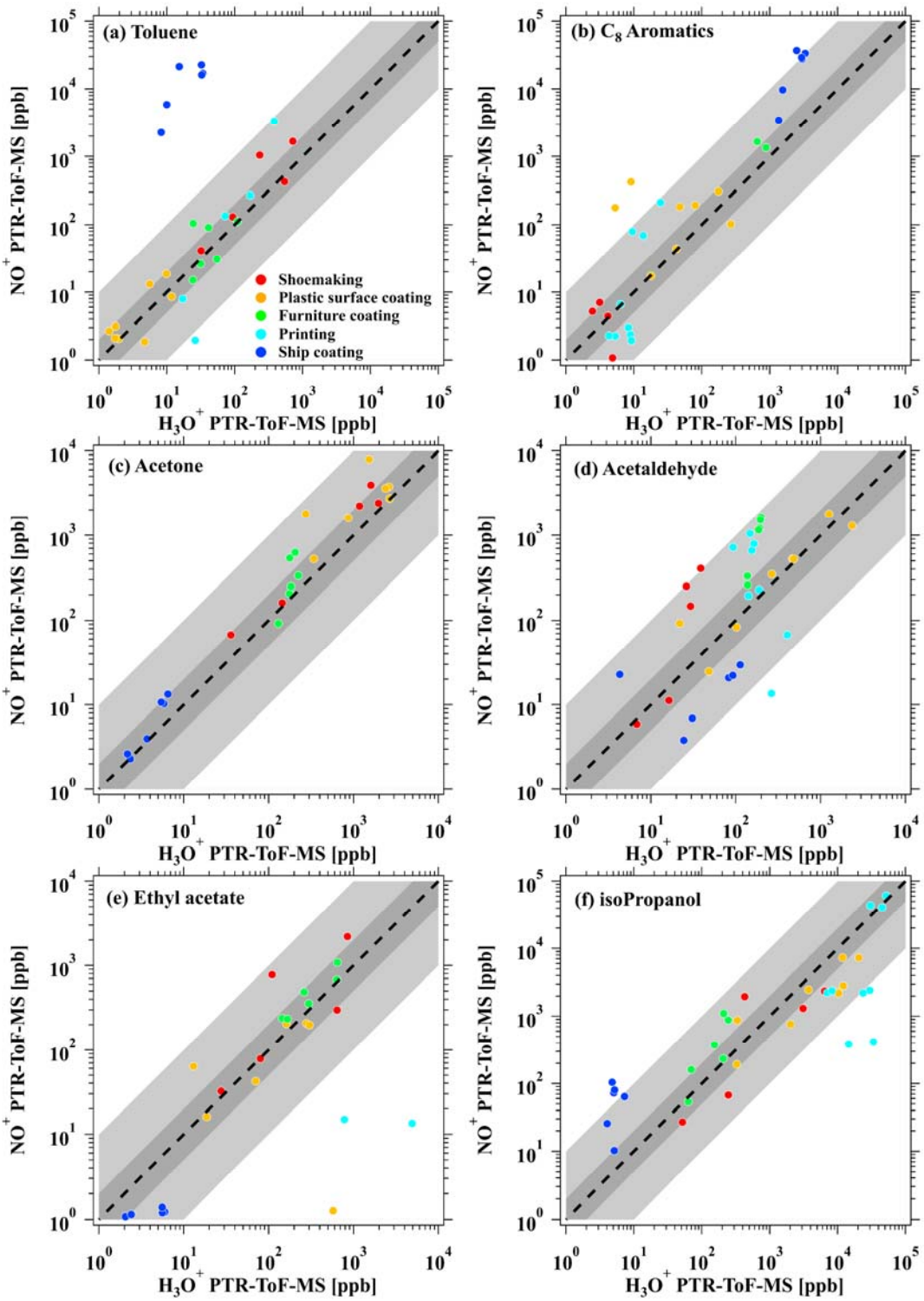

Figure S4. Scatterplot of (a) toluene, (b) C_8 aromatics, (c) acetone, (d) acetaldehyde, (e) ethyl acetate, and (f) isopropanol concentrations measured by H_3O^+ PTR-ToF-MS and NO^+ PTR-ToF-MS. The black dashed lines represent 1:1 ratio, and the shaded areas represent ratios of a factor of 2 and 10.

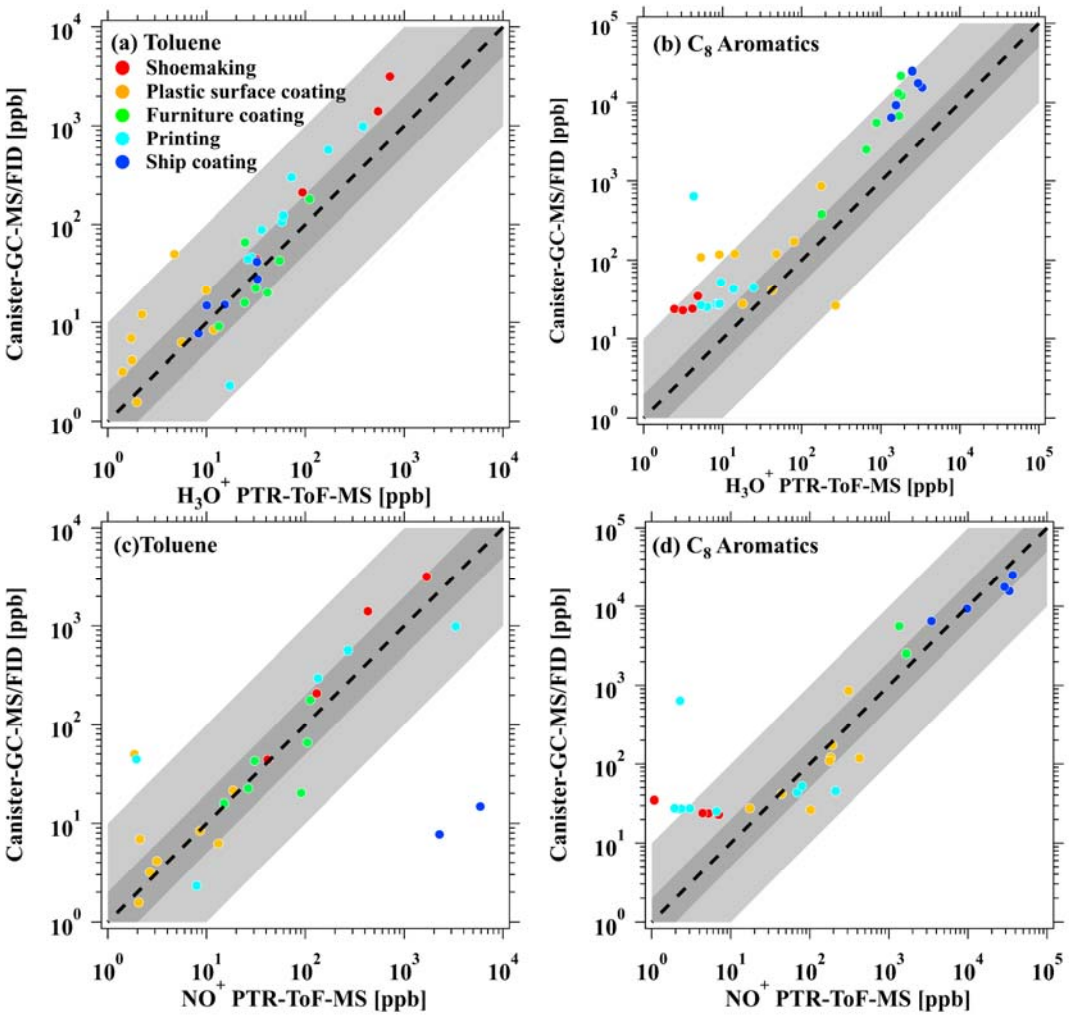

Figure S5. Scatterplot of (a) toluene and (b) C_8 aromatic concentrations measured by H_3O^+ PTR-ToF-MS and canister-GC-MS/FID. And (c) toluene and (d) C_8 aromatics concentrations measured by NO^+ PTR-ToF-MS and canister-GC-MS/FID. The black dashed lines represent 1:1 ratio, and the shaded areas represent ratios of a factor of 2 and 10.

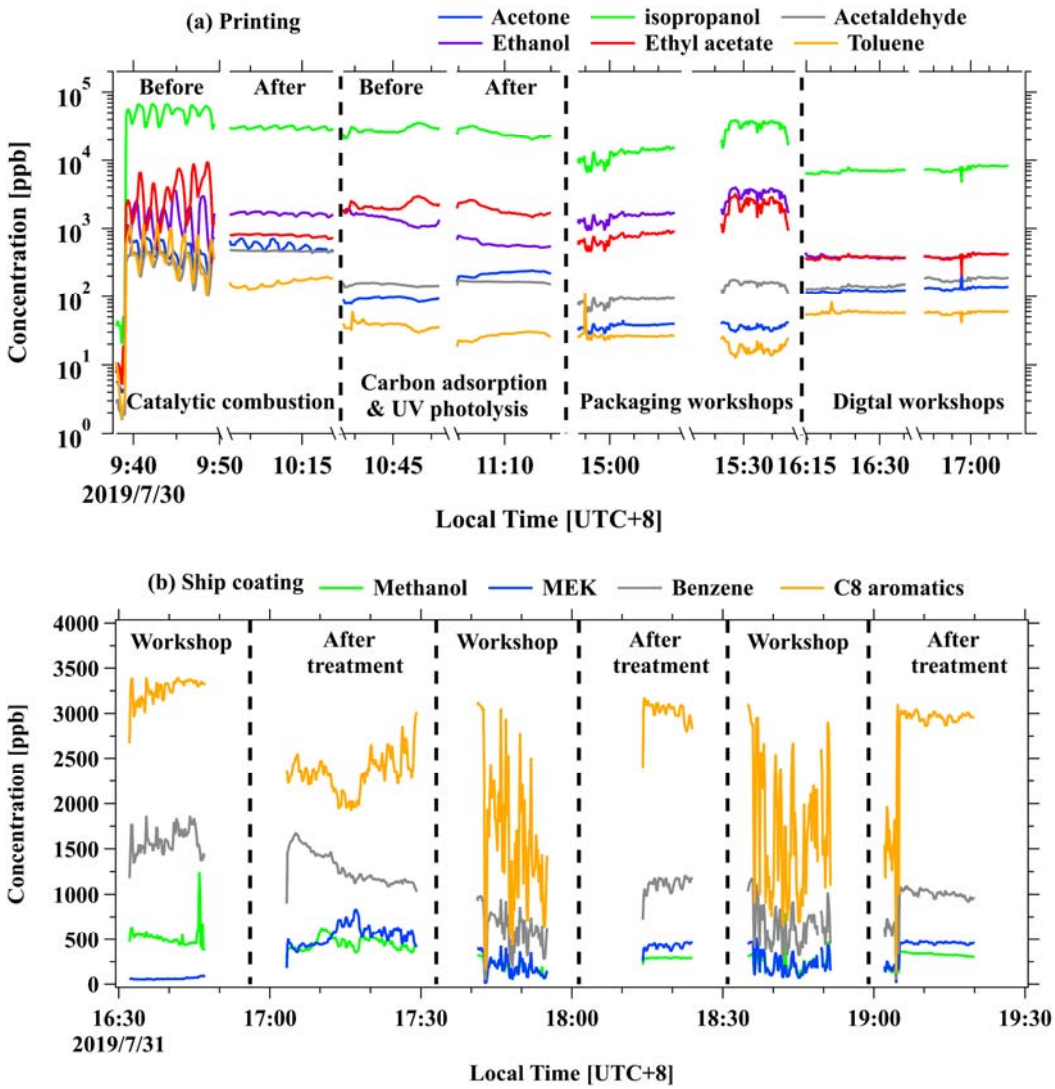

Figure S6. Real-time concentrations of representative ROGs from workshops, before and after the ROG treatment devices in (a) printing and (b) ship coating industries.

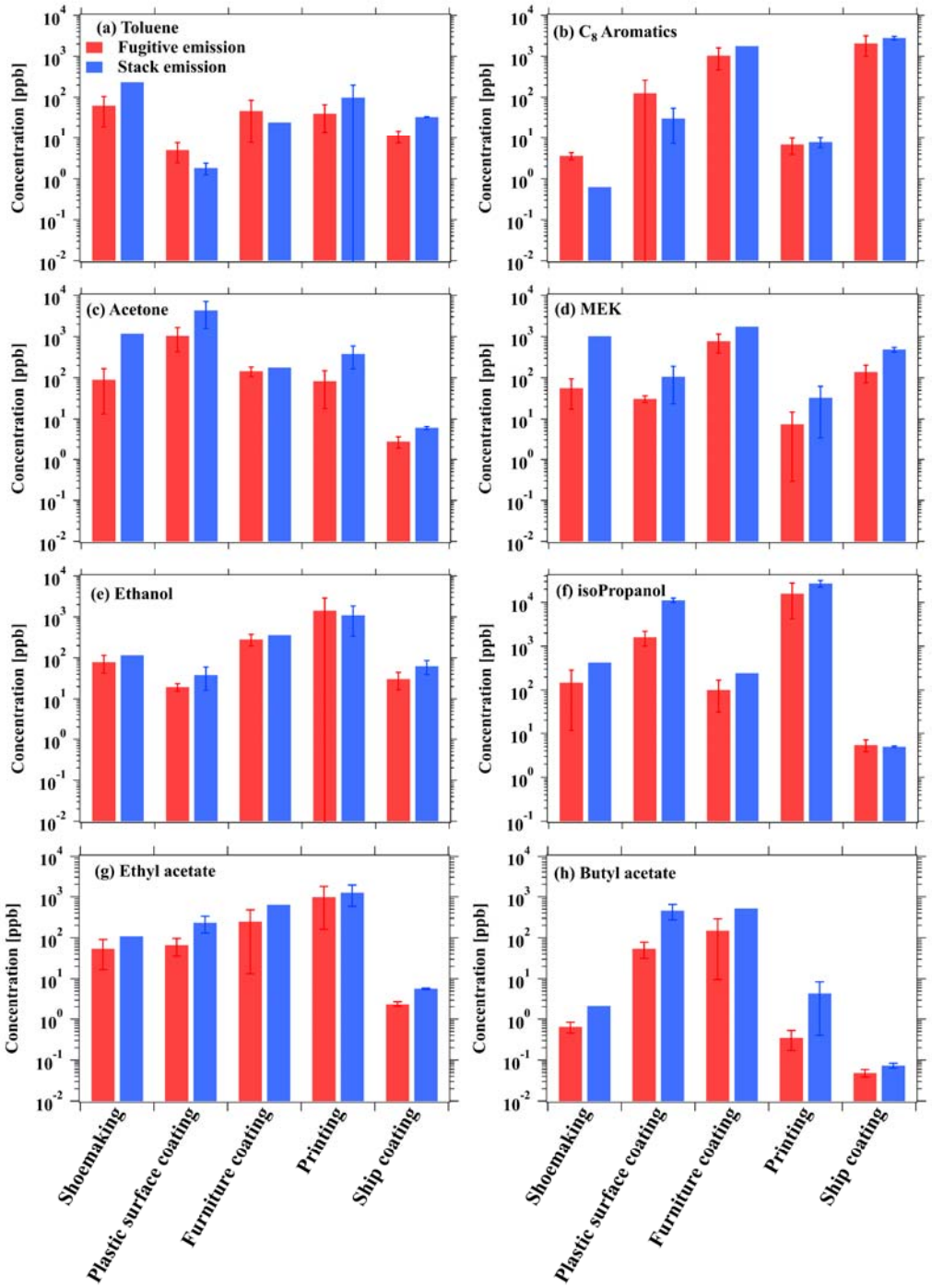

Figure S7. Average concentrations of (a) toluene, (b) C_8 aromatics, (c) acetone, (d) MEK, (e) ethanol, (f) isopropanol, (g) ethyl acetate, and (h) butyl acetate from both workshops (workshops emission) and after ROG treatment devices (stack emission) in shoemaking, plastic surface coating, furniture coating, printing, and ship coating industries, respectively. Error bars represent the standard deviations of the concentration.

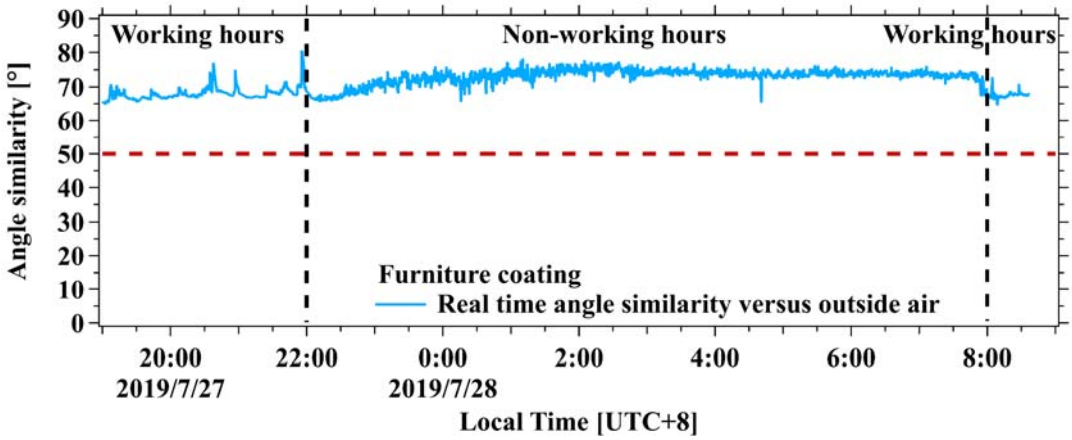

Figure S8. The θ angles of mass spectra among real-time concentrations versus outside air measurement in the furniture coating industry.

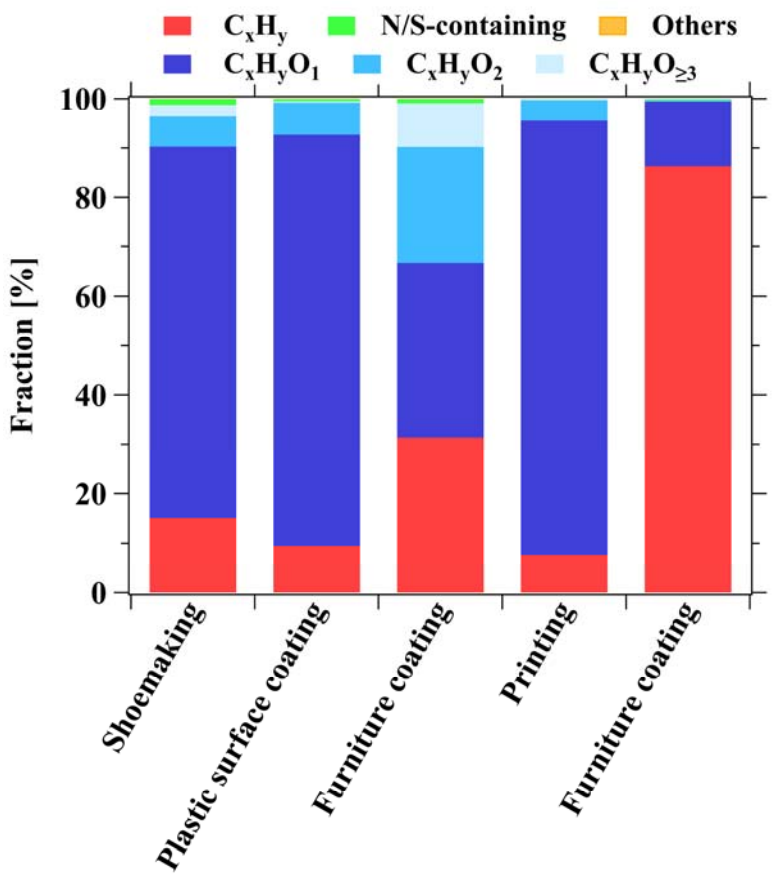

Figure S9. The fractions of different ROG categories measured by the PTR-ToF-MS from stack emissions across various industrial VCP sources.

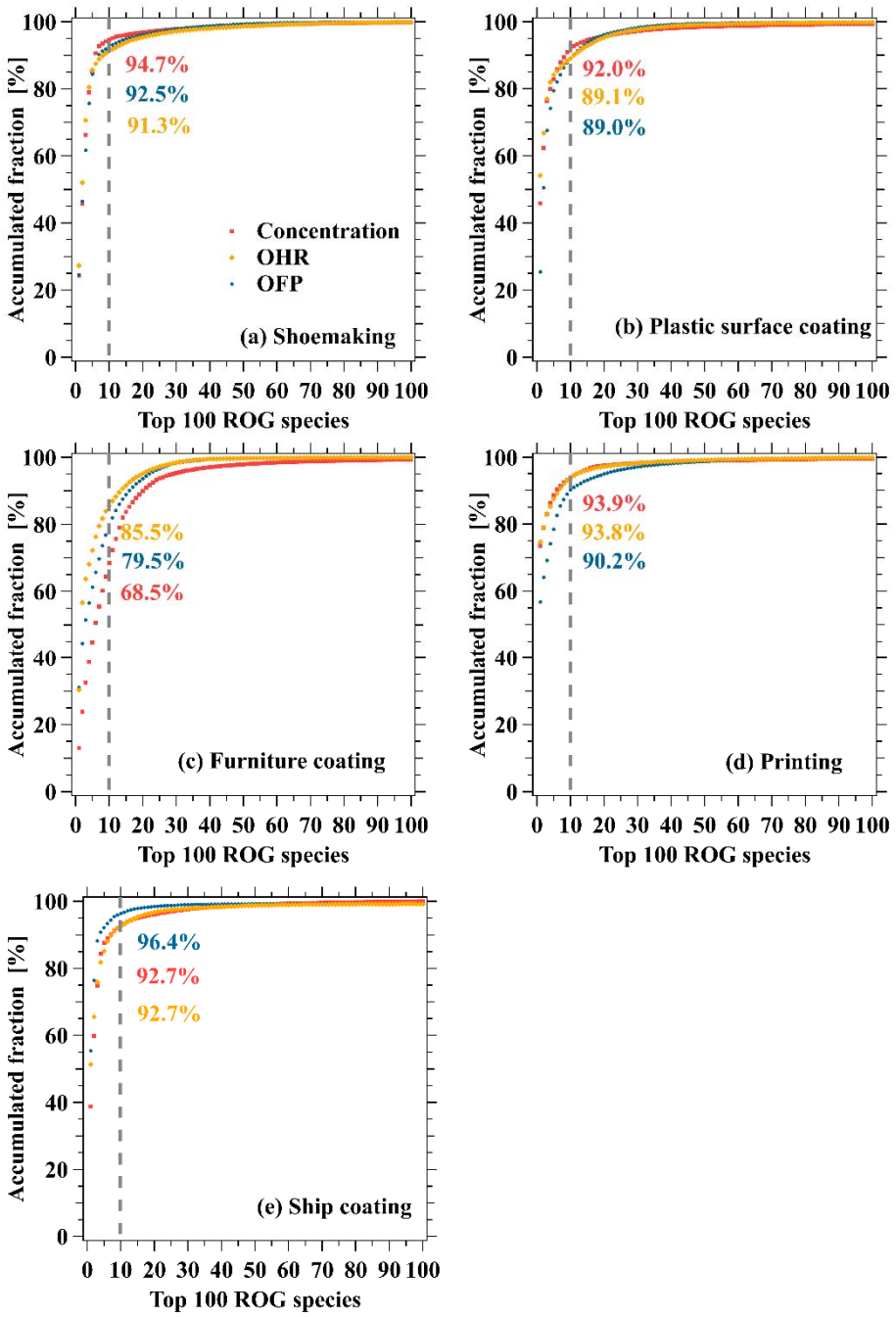

Figure S10. Accumulated fractions of the top 100 species in total ROG emissions, OHR, and OFP from (a) shoemaking, (b) plastic surface coating, (c) furniture coating, (d) printing, and (e) ship coating industries. The gray dashed lines represent accumulated fractions of the top ten in total ROG emissions, OHR and OFP.

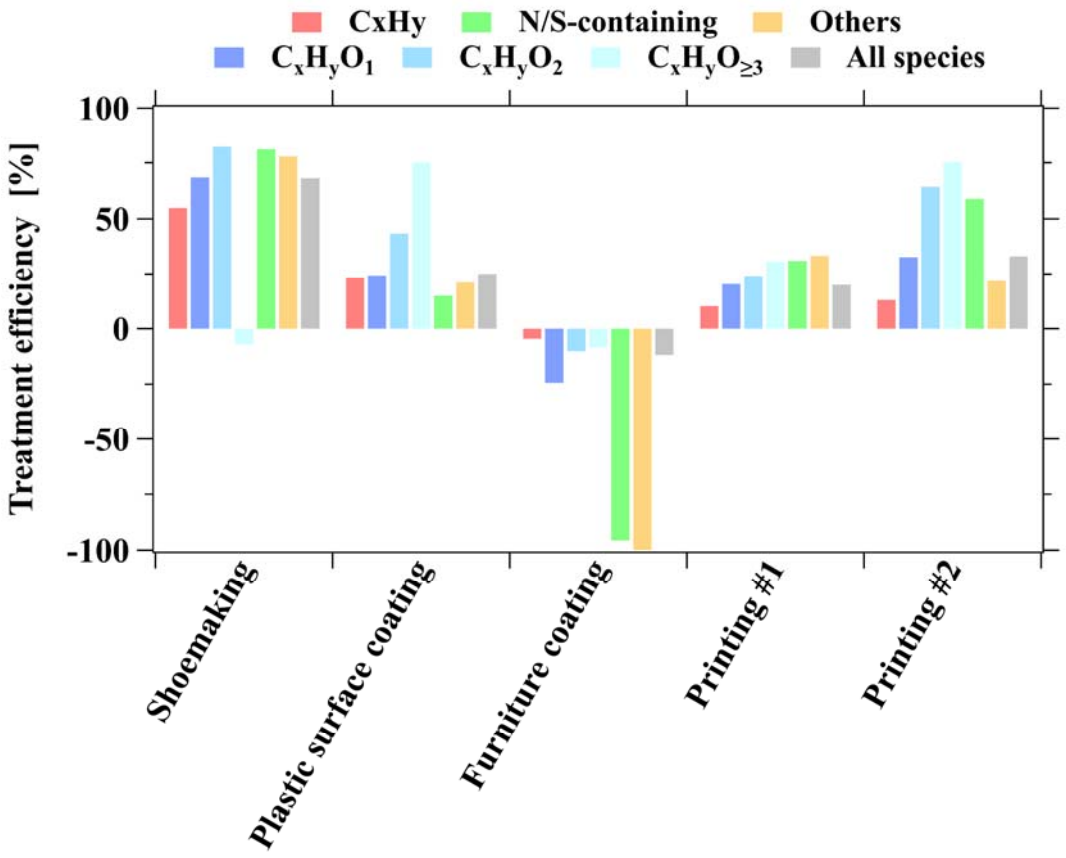

Figure S11. Treatment efficiencies of different ROG categories provided by treatment devices in various industrial VCP sources.

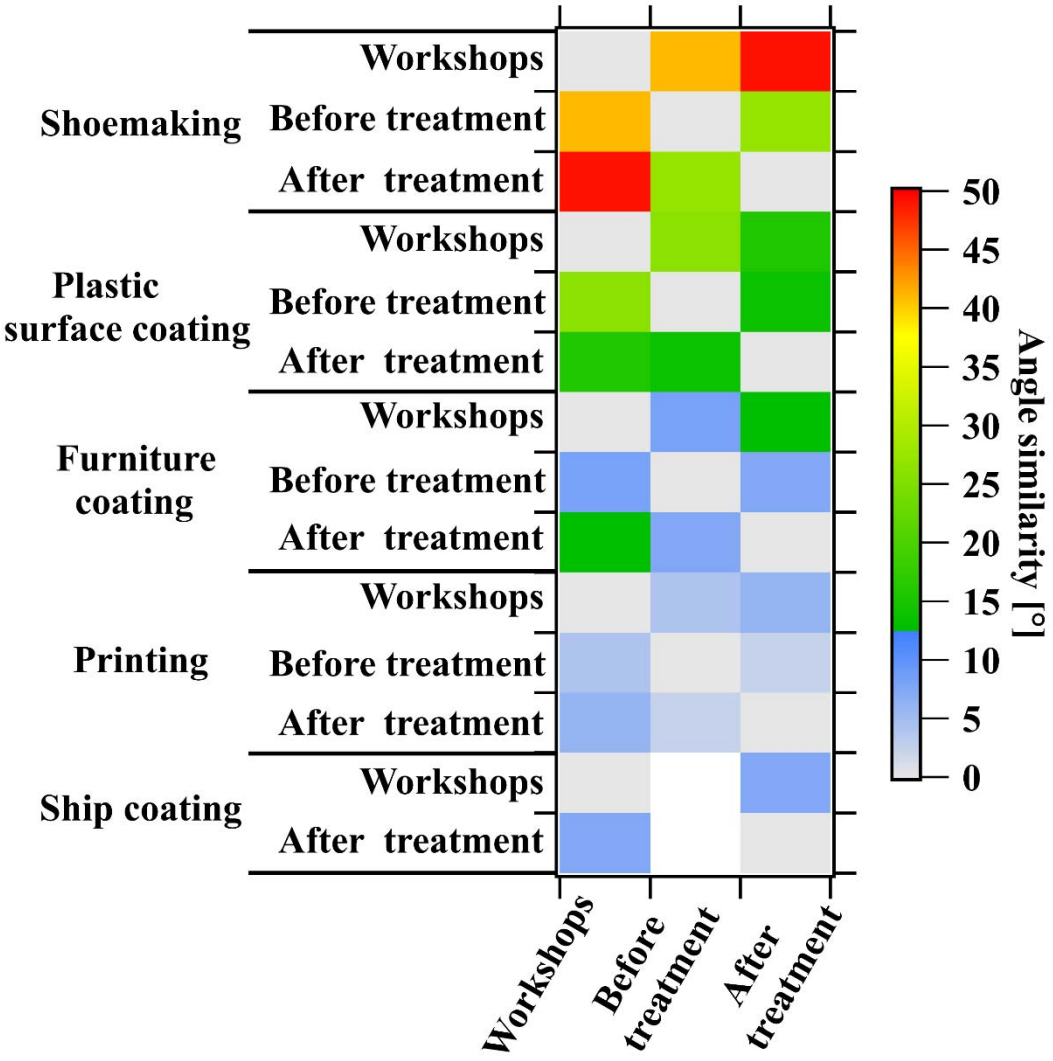

Figure S12. The θ angles among the mass spectra of workshops, before and after treatment in industrial VCP sources.

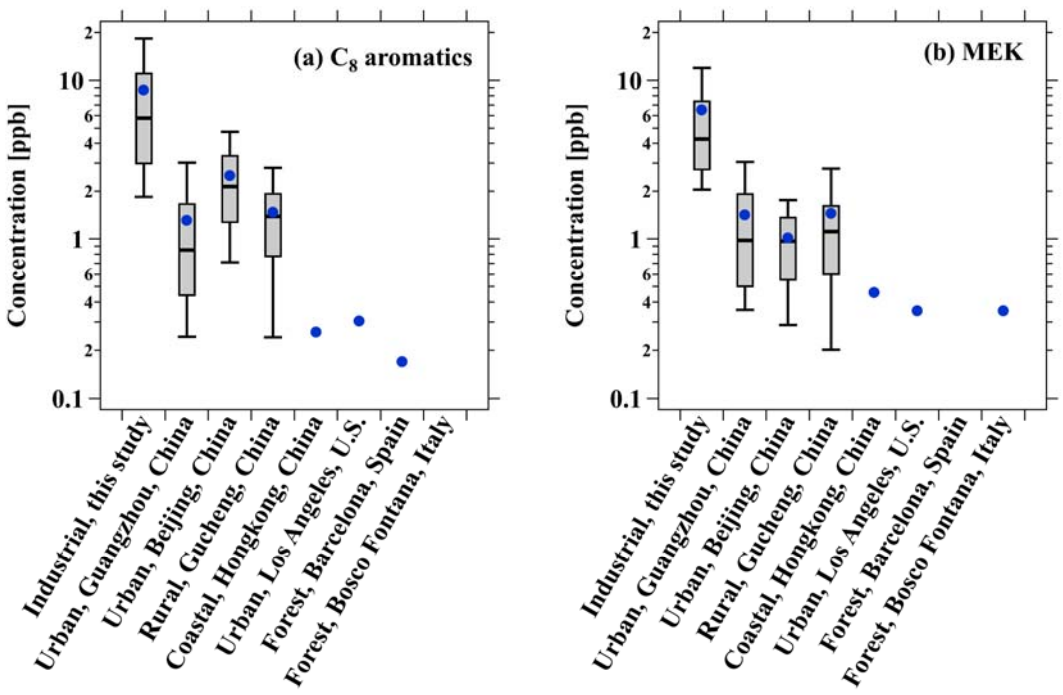

Figure S13. Boxplots of (a) C_8 aromatics and (b) MEK concentrations across the industrial site in this study and clean environments from previous studies.

References

Chen, Y., Yuan, B., Wang, C., Wang, S., He, X., Wu, C., Song, X., Huangfu, Y., Li, X. B., Liao, Y., and Shao, M.: Online measurements of cycloalkanes based on NO^+ chemical ionization in proton transfer reaction time-of-flight mass spectrometry (PTR-ToF-MS), Atmos. Meas. Tech., 15, 6935-6947, 10.5194/amt-15-6935-2022, 2022.

Estevan, C., Ferri, F., Sogorb, M. A., and Vilanova, E.: Characterization and evolution of exposure to volatile organic compounds in the Spanish shoemaking industry over a 5-year period, J Occup Environ Hyg, 9, 653-662, 10.1080/15459624.2012.725012, 2012.

Fang, L., Liu, W., Chen, D., Li, G., Wang, D., Shao, X., and Nie, L.: Source Profiles of Volatile Organic Compounds (VOCs) from Typical Solventbased Industries in Beijing (in Chinese), Environmental Science, 40, 4395-4403, 10.13227/j.hjkx.201901128, 2019.

Malherbe, L., and Mandin, C.: VOC emissions during outdoor ship painting and health-risk assessment, Atmospheric Environment, 41, 6322-6330, 10.1016/j.atmosenv.2007.02.018, 2007.

Wang, S., Yuan, B., Wu, C., Wang, C., Li, T., He, X., Huangfu, Y., Qi, J., Li, X. B., Sha, Q., Zhu, M., Lou, S., Wang, H., Karl, T., Graus, M., Yuan, Z., and Shao, M.: Oxygenated volatile organic compounds (VOCs) as significant but varied contributors to VOC emissions from vehicles, Atmos. Chem. Phys., 22, 9703-9720, 10.5194/acp-22-9703-2022, 2022.

Zhao, R., Huang, L., Zhang, J., and Ouyang, F.: Emissions characteristics of volatile organic compounds (VOCs) from typical industries of solvent use in Chengdu City (in Chinese), Acta Scientiae Circumstantiae, 38, 1147-1154, 10.13671 /j.hjkxxb.2017.0362, 2018.

Zheng, J., Yu, Y., Mo, Z., Zhang, Z., Wang, X., Yin, S., Peng, K., Yang, Y., Feng, X., and Cai, H.: Industrial sector-based volatile organic compound (VOC) source profiles measured in manufacturing facilities in the Pearl River Delta, China, Sci Total Environ, 456-457, 127-136, 10.1016/j.scitotenv.2013.03.055, 2013.

Zhou, Z., Deng, Y., Zhou, X., Wu, K., TAN, Q., Yin, D., Song, D., Chen, Q., and Zeng, W.: Source Profiles of Industrial Emission-Based VOCs in Chengdu (in Chinese), Environmental Science, 41, 3042-3055, 10.13227/j.hjkx.201912203, 2020.